Levodopa vs. deep brain stimulation: computational models of treatments for Parkinson's disease

Abstract

Parkinson's disease (PD) is a neurodegenerative disease affecting the dopaminergic neurons of the substantia nigra pars compacta, which alters the neurodynamics of the brain by decreasing the ability of the basal ganglia to faithfully translate motor cortex signals. Levodopa is a pharmaceutical used to treat PD which is converted to dopamine after crossing the blood brain barrier. The project expands upon a simplified model of the basal ganglia developed by David Terman & Jonathan Rubin (2004) in order to study the neurodynamics of levodopa treatment on a patient with PD. The results are compared to those of a PD model studying the effects of high frequency deep brain stimulation of the subthalamic nucleus.

Introduction

Deep brain stimulation (DBS) is thought to excite local neural targets, and the basal ganglia has been a target for DBS. (Garcia et al., 2003, Kringelbach et al., 2007) In particular, symptoms of Parkinson's Disease (PD) are alleviated by high (gamma, 30-80 Hz) frequency stimulation of the subthalamic nuclei (STN) (Wichman et al., 2006, Garcia et al., 2003), while the exact mechanism of alleviation remains unsolved. This result is seemingly contradictory to the inhibitory effects the STN has on movement; the STN sends excitatory signals to the internal segment of the globus pallidus (GPi), which tonically inhibits the ventroanterior/ventrolaterial nuclei of the thalamus (VA/VL). This in turn leads to signals from the motor cortex not being successfully transmitted to the VA/VL, with the overall effect inhibiting control of movement. This indicates that stimulation of the STN would have opposite effects than those observed, as one might logically conclude that excitation of an inhibitory center would further exacerbate the inhibitory effects. Using a computational model of the basal ganglia, Rubin et al. (2004) analyzed the differences in the dynamics of normal and Parkinsonian systems, and the resulting behavior from high frequency stimulation of the STN in PD. Their results reinforced the findings of Garcia et al. (2003), which indicated that stimulation of the STN silenced pathological oscillations and instead imposed a beneficial pattern of activity in the gamma band. This is consistent with a hypothesis positing the importance of the pattern of neuronal activity in addition to neuronal firing rate. Through analysis of the phase space behaviors of their model, Rubin at al. were able to demonstrate that Parkinsonian oscillation patterns in the STN/GPi network prevented proper response of the thalamus to motor signals, while the DBS-imposed tonic outputs restored fidelity to the network.

The computational model used by Rubin et al. (based on a model developed by Terman et al. (2002)) used a network of neurons from the STN, GPi, GPe (external segment of the globus pallidus), and the thalamus, with multiple neurons from each. The GPi and GPe both receive excitatory input from the STN, while there is interpallidal inhibition among GPe neurons, and the STN and GPi both receive inhibition from the GPe. Striatal input to the GPe and GPi (modified in Parkinson's disease due to elimination of dopaminergic inputs to the striatum) was treated as an applied current rather than a neuronal model. Sensorimotor input was modeled as a variable periodic step function. A reduced two-dimensional model of the network was then generated for phase space analysis.

Our first goal was to create a simplified version of this model in MATLAB while retaining the same qualitative behavior, using a single neuron from each brain structure (with a self-inhibiting GPe neuron). This was done in the hopes of expanding the model to include two striatal neurons (one each with excitatory D1 & inhibitory D2 receptors) to replace the applied current to the GPe and GPi as to more accurately represent the physiology. However, this was soon determined to be unfeasible, as multiple neurons proved necessary to generate the desired activity.

Our goal then became recreating the reduced model to model the progression of PD corresponding with the progressive death of dopaminergic neurons in the substantia nigra pars compacta. We then used the model to simulate L-DOPA (Levodopa) treatment. This model of pharmacological treatment (which essentially amounted to a "rescue" of normal activity) was then compared with the model of DBS treatment.

The Complete Model of Parkinson's Disease

The complete model of Parkinson's that Rubin used was based off of physiological connections between the structures of the basal ganglia involved in Parkinson's Disease and the thalamus. Each structure is modeled as a set of reduced Hodgkin-Huxley neurons, each with leak current and ion channel terms for sodium, potassium, and calcium (see Appendix A for the equations used).

The input from the striatum to the GPe and GPi was modeled as a constant for simplification. The sensorimotor input to the thalamus is modeled as a repeating Heaviside equation with a period of ρ_{SM}, and pulse duration of δ_{SM}. The current assigned to deep brain stimulation applied to the subthalamic nucleus was modeled in the same way as the sensorimotor input, as a repeating Heaviside function with a designated period and pulse duration.

In addition, there were terms for the current applied to each neuron from synapses with neurons from other structures. These synaptic currents are governed by differential equations dependant on the presynaptic neuron's voltage. For instance, the STN has an inhibitory input current from the GPe. In Rubin's model there were sixteen STN, GPe and GPi neurons, and two thalamic neurons, and the number of connections between neurons of different structures was physiologically relevant. See **Figure 1** for the connections between structures that were modeled by Rubin et al.

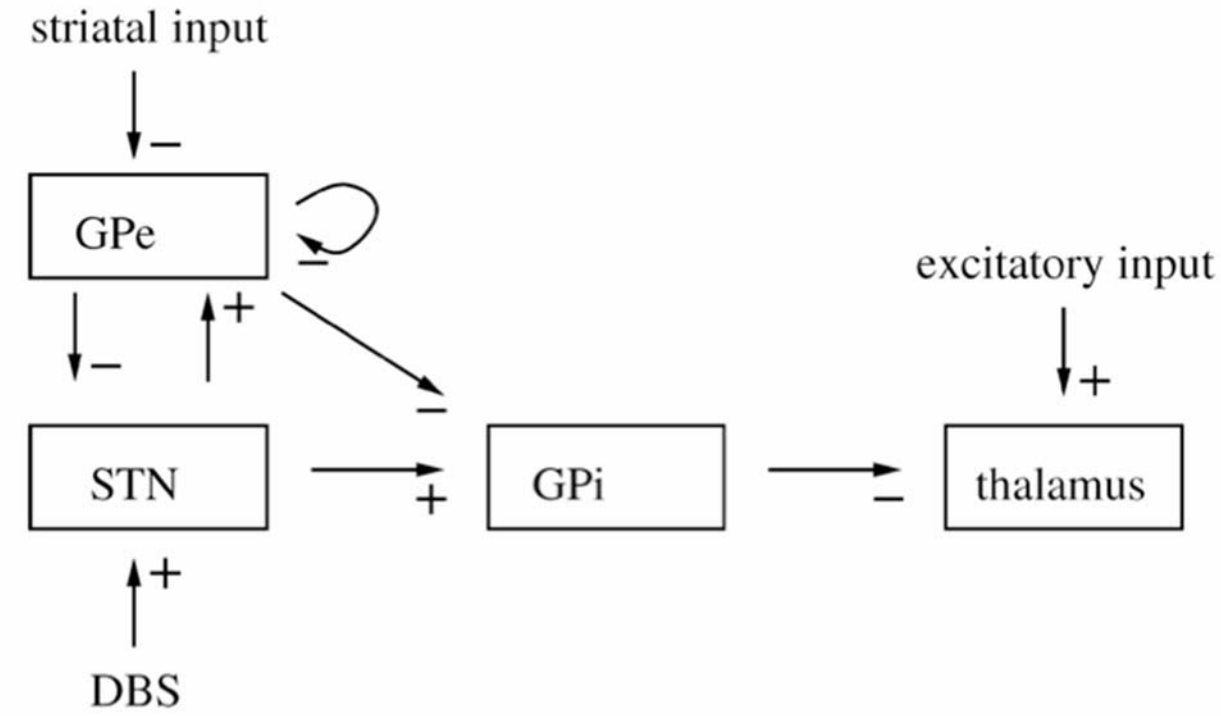

Figure 1: *Connections between deep brain structures modeled in the complete system of equations by Rubin et al.*

This network produced random spiking in the STN to model normal firing patterns in a healthy brain, seen in the figure on the left below. In order to model Parkinson's disease, the striatal input to the GPe and GPi were increased, and the conductance of the inhibition from the GPe to itself was decreased. This caused the neurons to synchronize and produce the firing patterns seen on the figure below and to the right. The increased input to the GPe and decreased inhibition led to a pattern of gaps in the GPe firing. These gaps led to decreased inhibition of the

GPi, causing a pattern with areas of increased firing activity and areas with decreased firing activity. Because the GPi inhibits the thalamus, these areas of increased firing inhibit sensorimotor input to the thalamus from translating into thalamic neuron spiking. This means that desirable motor input is not translated into thalamic spiking, and the patient's muscles do not receive the signals needed to perform motor functions properly.

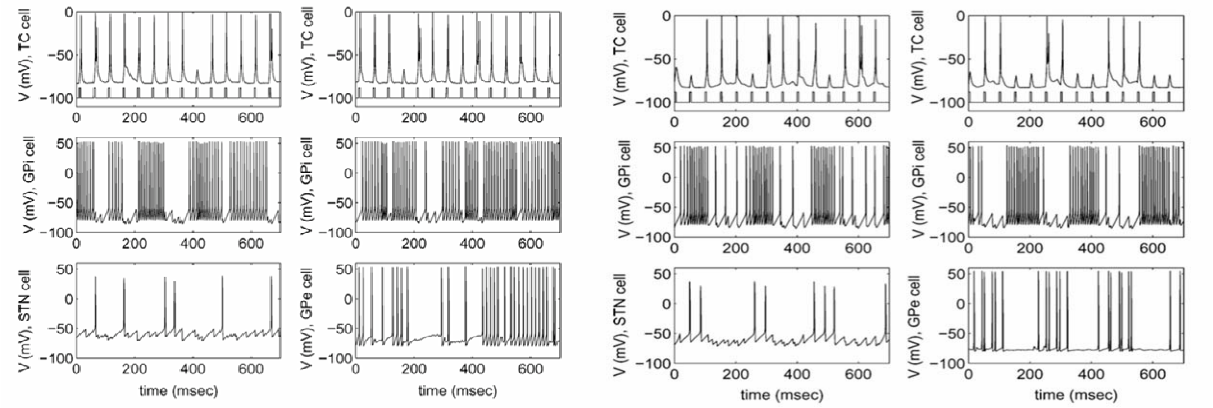

Figure 2: *Simulated Neuronal firing patterns in a) a healthy patient b) a Parkinson's patient.*

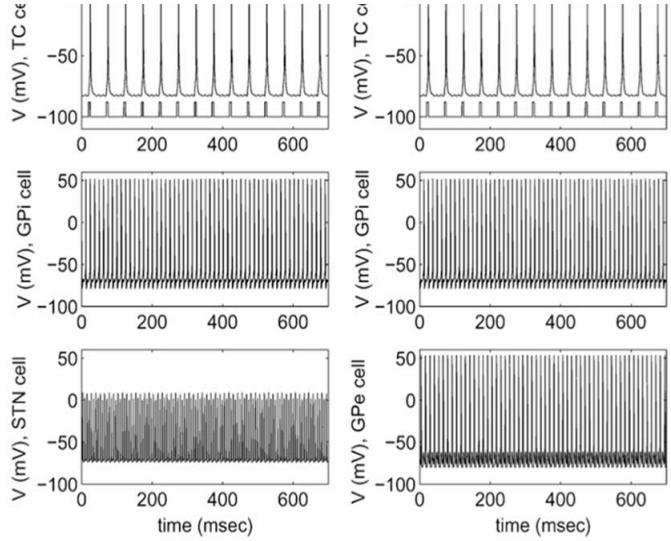

Figure 3: *Simulated neuronal firing patterns in a Parkinson's patient receiving DBS treatment.*

The same results could not be produced with a network of structures modeled with single neurons. That is because not all of the neurons fire in exactly the same way, as can be seen in **Figure 2**. The importance of the network is the synchonicity of the STN neurons that develops from the interactions between multiple neurons with the same properties but different connections to neurons from other structures.

When DBS is introduced into the model, it forces the STN to fire rhythmically. Because the STN sends excitatory input to the GPe, DBS induces increased and rhythmic firing of the GPe, as can be seen in **Figure 3**. The GPi fires less frequently due to the increase in inhibitory input from the GPe, and sensorimotor input is faithfully translated into thalamic neuron spiking.

The Reduced Model of Parkinson's

While the results from the full Rubin model matched with expectations, it was difficult to analyze in phase space as it was multidimensional. Therefore, Rubin et al. reduced the model to a two-dimensional model of the calcium inactivation variable (now w) and voltage (V), ignoring the sodium and potassium currents in the full network (I_{Na} & I_K) and increasing the conductance of the transient calcium current (g_T). Further analysis by Rubin et al. determined that this could be done because the calcium current effectively replaced the sodium current in the full network in contributing to the spiking behavior. I_{SM} and I_L were kept in the same form as in the full

network model. In addition, the synaptic input is now modeled as an external current ($I_{Gi\rightarrow Th}$). This can be justified as the high frequency stimulation from the GPi to the thalamus was at a much higher frequency than the sensorimotor input to the thalamus in the full model during normal and DBS activity, which allows those situations to be modeled with a constant current. The Parkinsonian case showed patterned oscillatory activity with periods of essentially no activity followed by high frequency bursts. This could then be modeled as a Heaviside input function. The general equations for the reduced model are listed in **Appendix B**.

We attempted to recreate the Rubin model exactly using the provided parameters; however, once the equations were placed into MATLAB, we discovered problems with the parameters provided in their report. As the equation of the V-nullcline was of the form

$$v' = -(I_L + I_T) / C_{Th} - I_{Gi\rightarrow Th} + I_{SM}$$
$$I_T = g_T * p_\infty(v) * w * (v - E_T)$$

We should obtain a V-nullcline with a vertical asymptote at E_T, which Rubin et al.'s paper defined to be zero. From **Figure 4**, this was clearly not the case in their nullclines. However, as the activity of the neurons appeared to not surpass 0 mV (except in Parkinsonian activity), we simply modified the provided equations and parameters until we obtained topologically equivalent nullclines in the normal case (**Figure**). This was done under the assumption that itwe could then generate similar activity through trial and error with initial conditions. The equations and parameters we used are listed in **Appendix B**, along with their original counterparts in **Appendix A**. Our modified equations led to a longer spiking time, and thus the periods for our external current were extended to give the same qualitative spiking behavior in the normal case (**Figure 5b**).

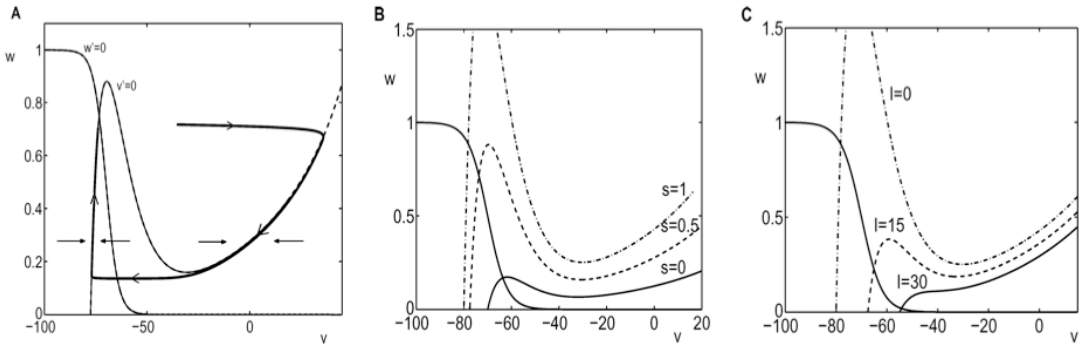

Figure 4: *Nullclines for the reduced thalamic neuron model from Rubin's paper. (a) The bold line shows the response to a depolarizing input (b) nullclines when the conductance between GPi and the thalamus is 0.8 (c) nullclines when s = 1.*

To model normal behavior, we used $i_{SM} = 2$, $\rho_{SM} = 13$, and $\delta_{SM} = 72$, with $s_{Gi} = 0.5$. As we can see in **Figure 5** below, the spiking behavior we obtained in the normal case is qualitatively similar to Rubin et al.'s published results. A notable difference is our spiking trailing the sensorimotor input about 50 ms, but this can be attributed to the longer time constants mentioned above. The phase space also showed similar activity as the original model, with the trajectory less closely following the V-nullclines due again to our longer time constant. Regardless, it can be seen that each sensorimotor signal elicits a spike.

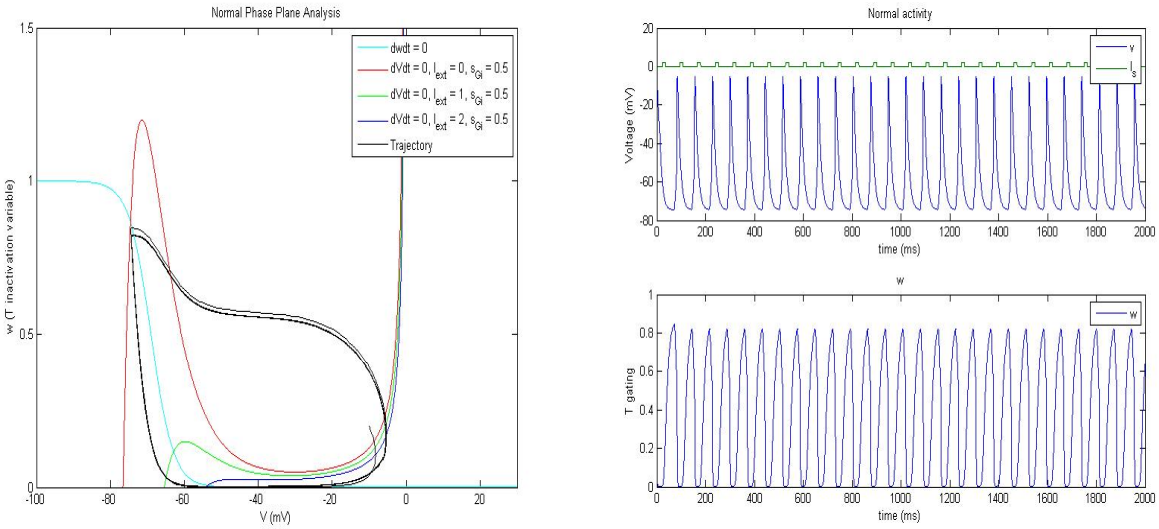

Figure 5: *Thalamic neuron firing in a healthy person obtained by simulating the reduced model. (a) Limit cycle (b) Neuron spiking behavior.*

For modeling DBS behavior, the parameters were kept the same as in the normal case except with s_{Gi} raised to 0.87. This was to simulate high frequency DBS leading to more tonic inhibition of the thalamus by the GPi, as described in Rubin et al.'s report. **Figure 6b** shows the spiking behavior, which is very similar to that of the normal situation. The trajectory is somewhat compressed compared to the normal case (shown in the left figure below), which is consistent with the original results. Again, each sensorimotor signal is faithfully translated as a spike. **Figure 7** below shows the dependence of the limit cycle on s_{Gi} * g_{GiTh}, showing an ideal "sweet spot" range which DBS generated activity must fall within. When it becomes too high, the inhibition is enough to completely keep the thalamic neurons from firing, blocking motor signals altogether.

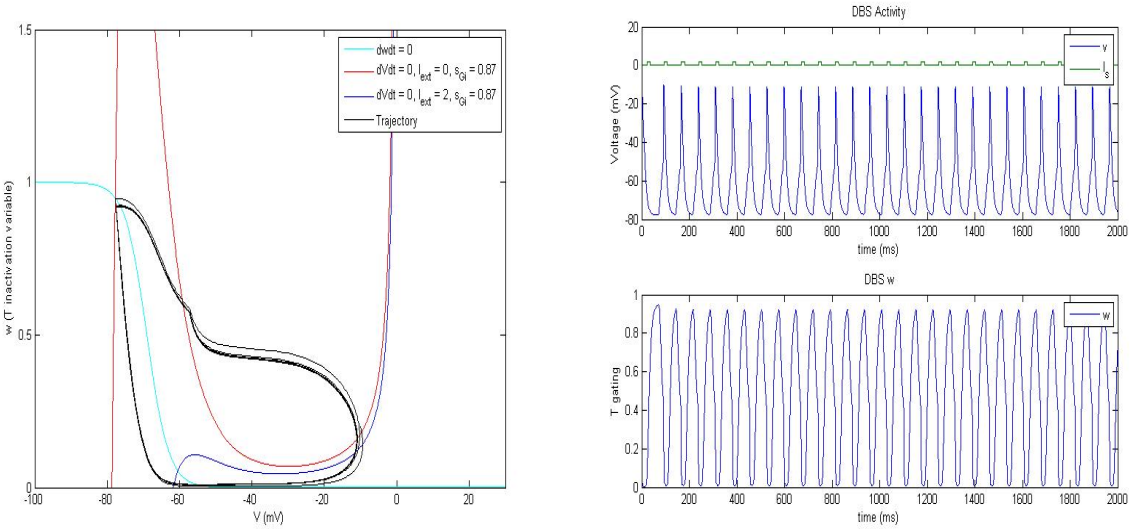

Figure 6: *Thalamic neuron firing in a Parkinson's patient receiving DBS treatment obtained by simulating the reduced model. (a) Limit cycle (b) Neuron spiking behavior.*

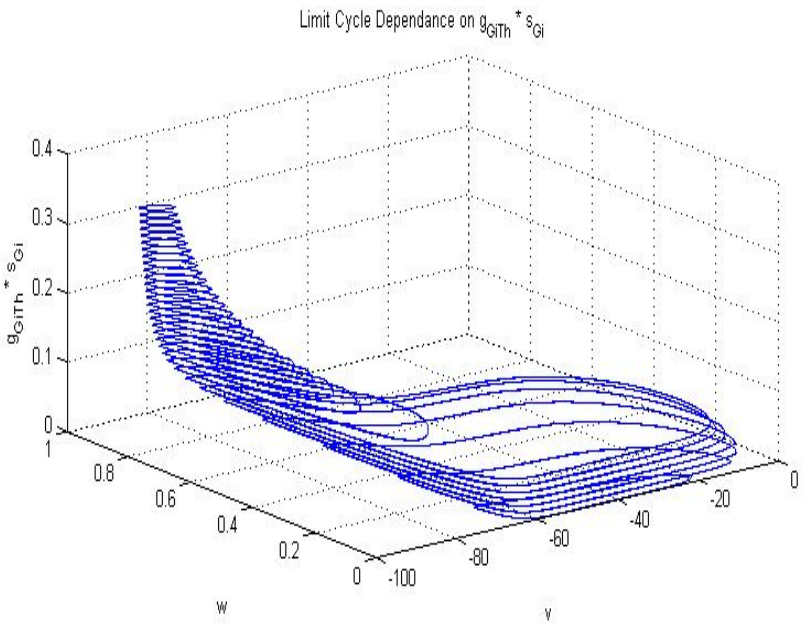

Figure 7: *The limit cycle changes drastically based on the value of g*s. There is only a small range of values for g*s where the limit cycle is physiologically reasonable.*

In the Parkinsonian case, we modified s_{Gi} to be

$$s_{gi}(t) \text{ for PD} = H(\sin(2 * \pi * t / \rho_I)) * [1 - H(\sin(2 * \pi * (t + \delta_I) / \rho_I))]$$

This is where our results show significant divergence from Rubin et al.'s. While their chosen synaptic input created generated four distinct limit cycles (**Figure 8**), we were not able to create topologically equivalent behavior. This may once again be attributed to our modified time constants. However, we were able to generate behavior that provides an explanation for Parkinsonian behavior regardless.

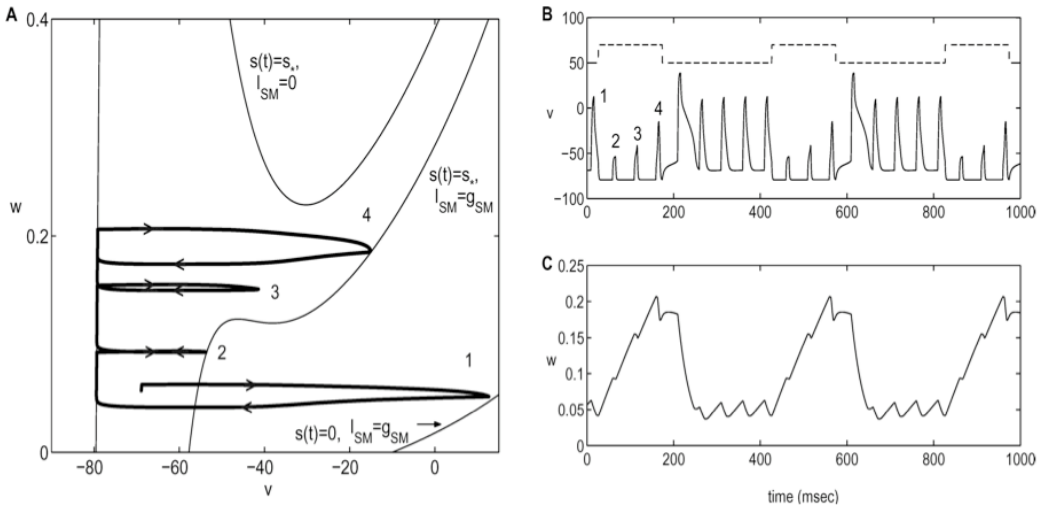

Figure 8: *The Parkinson's case of the reduced thalamic neuron model. (a) Nullclines and limit cycles (b) Thalamic voltage in terms of time (c) Gating variable in terms of time.*

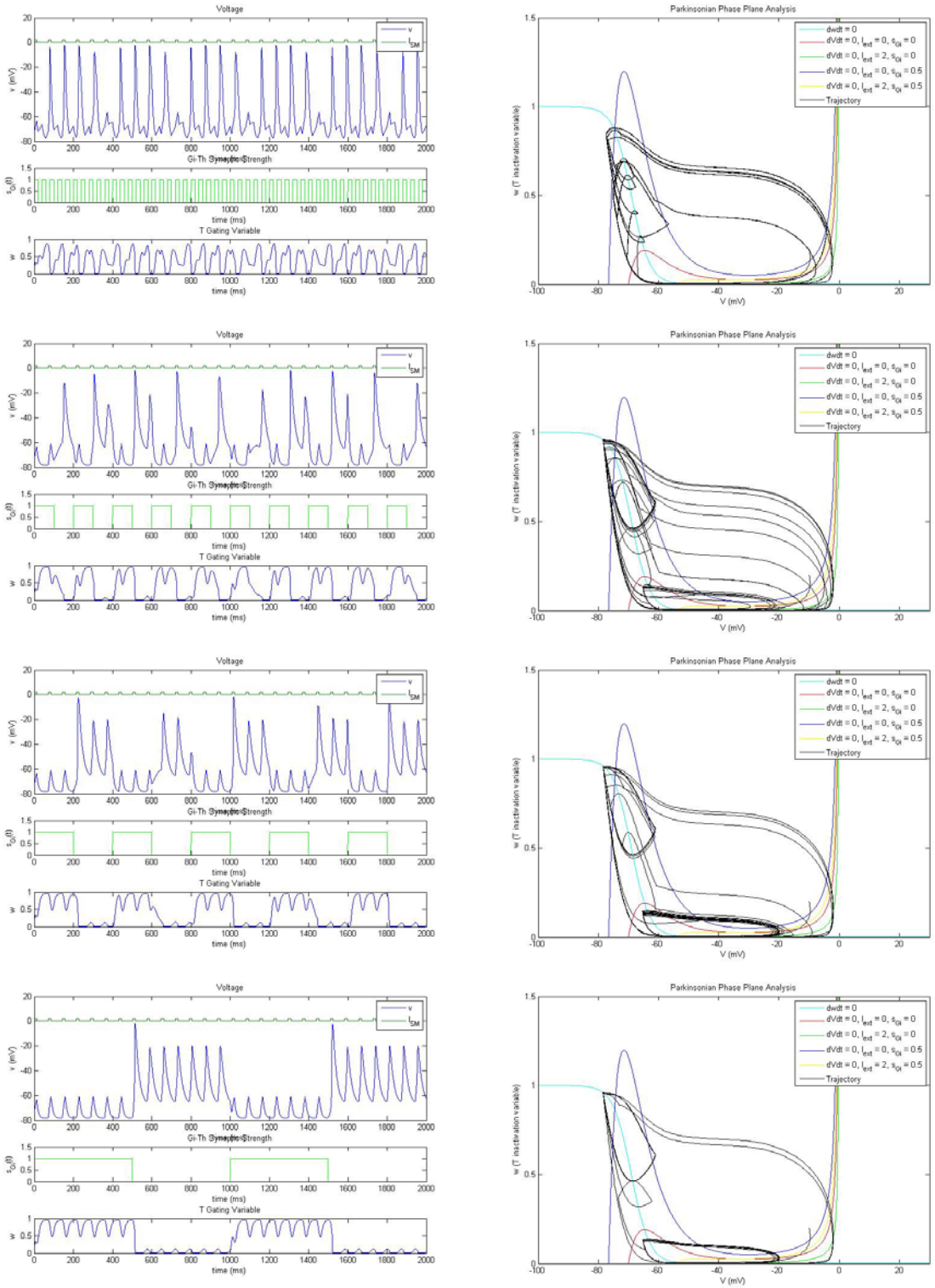

Figure 9: *The progression of Parkinson's disease is shown from (a) to (h). As the disease progresses, there develop times where the GPi fires too much and inhibits the thalamus such that the sensorimotor input to the thalamus does not cause the neuron to fire.*

Figure 9 shows a series of spiking behavior with increasing periods of synaptic inhibition. Initially, we use a high frequency synaptic input, which is the physiological basis of our assumption of a constant s_{Gi} in the normal and DBS cases. With this input, we can see that the sensorimotor signals are still translated with fairly high fidelity, missing only every fifth spike. The accompanying phase diagram shows a main limit cycle which diverges with the missed spike.

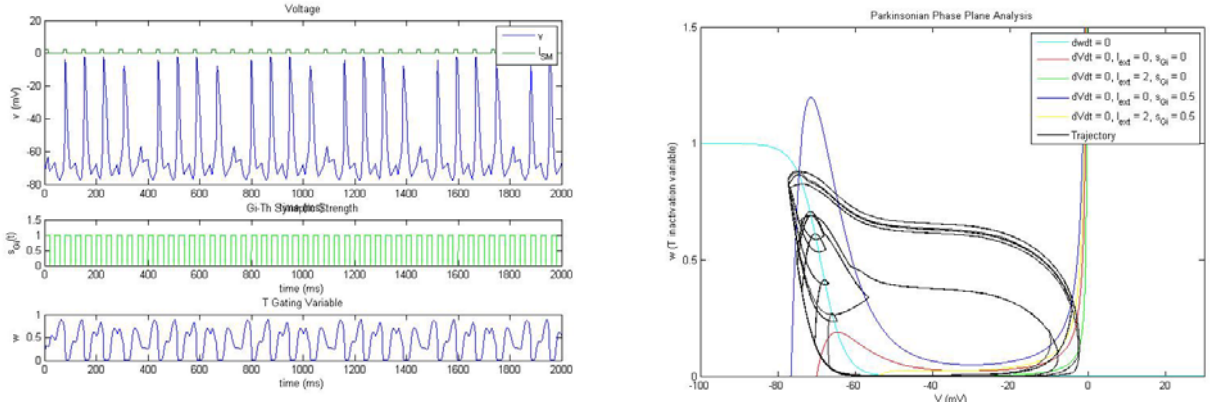

Figure 10: *The proposed thalamic spiking behavior on a Parkinson's patient receiving Levodopa. (a) Thalamic spiking (b) Thalamic limit cycle.*

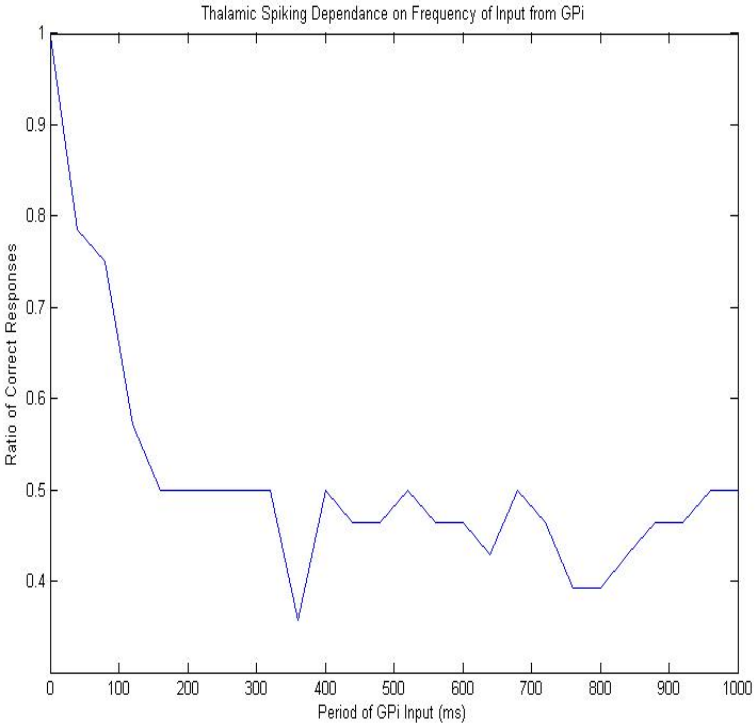

Figure 11: *The effect of the frequency of the Heaviside input from the GPi on thalamic spiking "misses".*

Once the synaptic input becomes more oscillatory, we see significant increases in missed spikes. This may model the progression of PD well, with the progressive death of dopaminergic neurons in the SNpc causing the gradual change in activity in the downstream GPi. In the phase diagrams we can see trajectories which eventually show multiple distinct limit cycles, though never to the clean degree (with four distinct limit cycles) seen by Rubin et al. **Figure 11** shows the progression of spike misses with longer periods of synaptic input. This graph assumes that the ratio of spike duration to period length was one half.

Modeling Levodopa Treatment With the Reduced Model

Levodopa was modeled as the near to perfect translation of sensorimotor input into thalamic spiking as seen in **Figure 10**. In this case, the input from the GPi to the thalamus is given by a Heaviside function with a short period of 40ms, and pulse duration of half the period length. As can be seen from the graph of thalamic spiking in terms of period of GPi input, the shorter the period of GPi input the more the thalamic neurons spike when excited by sensorimotor input.

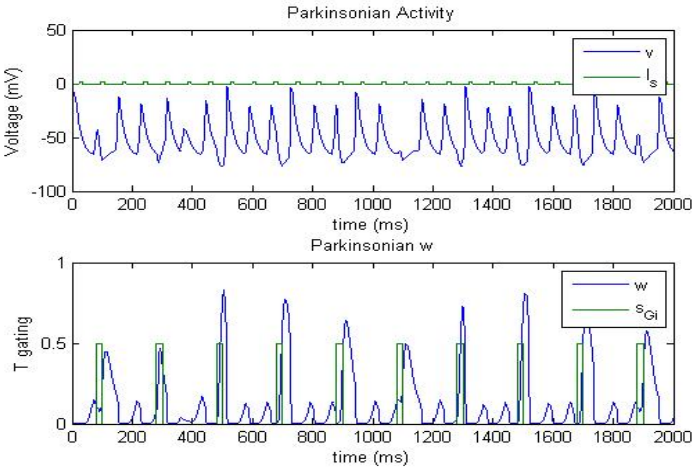

Figure 12: *The effect of varying the input from the GPi to the thalamus such that the ratio of the pulse duration to the period is less than ½.*

Sensorimotor input is also more faithfully translated when the pulse duration is decreased and there are long periods of time when there is no GPi input, as can be seen in **Figure 12**. The stimulation period used here was 200ms with a spike period of 20ms. The possible physiological implications of this result are discussed below.

Discussion

The progression of Parkinson's as proposed here occurs when there are bursts of high frequency firing of the GPi, which inhibits the thalamus, shown here as the pulses of the Heaviside function. From this effect thalamic "spike misses" occur when sensorimotor input is not faithfully translated due to thalamic inhibition from the GPi. Spike misses are frequent once the pulse duration of GPi input to the thalamus is longer than 40ms and the ratio of pulse duration to Heaviside period is one half.

However, as shown in **Figure 12**, we noticed that shorter periods of GPi inhibition when compared with the entire stimulation period may also be conducive to spiking. This is consistent with the idea that less inhibition overall would allow faithful reproduction of signals. Physiologically, this may be consistent with pallidotomy as a treatment for Parkinson's, further lending credence to our model's accuracy.

In this paper was a proposed model for modeling thalamic neuron spiking in response to Levodopa treatment. In order to further verify the physiological validity of this model, it would be necessary to model Rubin's full system of neurons and add a set of neurons for the striatum and connections to the GPi and GPe neurons. Rubin's current complete model models striatal input as constant, which is an oversimplification of the main input to the system, and the value that changes due to the onset of Parkinson's disease. This model uses the assumption that Levodopa treatment simply reverses the progression of Parkinson's Disease by replacing the dopamine source lost with the Substantia Nigra Pars Compacta. Obviously, this is likely a gross oversimplification, and a good way to implement the more complex interactions Levodopa likely undergoes with the basal ganglia is a key area to explore in the future. A method to take into account dosage and longer time scales must also be determined in order to model the progression between on- and off-periods of Levodopa medication.

Due to our changing of parameters from the Rubin model, our systems are obviously not representative of true biological systems. However, it is important and encouraging to note that the behaviors obtained may still explain Parkinsonian activity, despite our model's obvious differences from the Rubin model. Therefore, it is likely that while our model probably does not represent the true activity in Parkinson's Disease, the general hypothesis of patterned oscillatory activity in the GPi leading to impaired spiking appears to hold. The most important future work to be done relating to our model is then to verify that this relationship continues to hold with more complex and accurate full models. If the circuit ever becomes fully elucidated and accurately modeled, it will likely become possible to obtain individualized parameters for specific patients. This may allow physiologically accurate simulations to be run for both L-DOPA and DBS treatments for individual patients, optimizing treatment options with far less trial and error.

Appendix A:

Full Model Equations:

Thalamic Neurons

$C_m * v'_{Th} = -I_L - I_{Na} - I_K - I_T - I_{Gi\rightarrow Th} + I_{SM}$

$h'_{Th} = (h_\infty(v_{Th}) - h_{Th}) / \tau_h(v_{Th})$

$r'_{Th} = (r_\infty(v) - h_{Th}) / \tau_r(v)$

$I_T = g_T * p_\infty(v_{Th}) * r_{Th} * (v_{Th} - E_T)$

$I_{SM} = i_{SM} * H(\sin(2 * \pi * t / \rho_{SM})) * [1 - H(\sin(2 * \pi * (t + \delta_{SM}) / \rho_{SM}))]$

STN Neurons

$C_m * v'_{Sn} = - I_L - I_K - I_{Na} - I_T - I_{Ge\rightarrow Sn} + I_{DBS}$

GPe/GPi Neurons

$C_m * v'_{Ge} = - I_L - I_K - I_{Na} - I_T - I_{Sn\rightarrow Ge} - I_{Ge\rightarrow Ge} + I_{app}$

Synaptic currents

$I_{\alpha\rightarrow\beta} = g_{\alpha\rightarrow\beta} * [v_\alpha - E_{\alpha\rightarrow\beta}] * \Sigma s_\alpha$

$s'_\alpha = A_\alpha * [1 - s_\alpha] * H_\infty(v_\alpha - \theta_\alpha) - B_\alpha * s_\alpha$

Appendix B:

Reduced Model Thalamic Neurons:

$v' = -(I_L + I_T) / C_{Th} - I_{Gi\rightarrow Th} + I_{SM}$

$w' = \varphi(w_\infty(v) - w) / \tau_h(v)$

$I_{Gi\rightarrow Th} = g_{Gi\rightarrow Th} * s_{Gi} (v - E_{Gi\rightarrow Th})$

Equations & Parameters for Reduced Model:
g_{GiTh} Original = 0.8
g_{GiTh} Modified = 0.079
$A_h = 0.128 * \exp(-(V + 46) / 18)$
$B_h = 4 / (1 + \exp(-(V + 23) / 5))$
p_∞ Original $= 1 / (1 + \exp(-(V + 60) / 6.2))$
p_∞ Modified $= 1 / (1 + \exp(-(V + 40) / 9.3))$
w_∞ Original $= 1 / (1 + \exp((V + 84) / 4))$
w_∞ Modified $= 1 / (1 + \exp((V + 69) / 3))$
$\tau_h = 1 / (A_h(V) + B_h(V))$

References:

Garcia, L., D'Alessandro, G., Bioulac, B., Hammond, C. (2003). "High-frequency stimulation in Parkinson's disease: more or less?" Trends in Neurosci. 28: 209-16

Kringelbach, M. L., Jenkinson, N., Owen, S. L. F., Aziz, T. Z. (2007). "Translational principles of deep brain stimulation." Nature Rev. Neurosci. 8: 623-35

Rubin J., Terman D. (2004). "High frequency stimulation of the subthalamic nucleus eliminates pathological thalamic rhythmicity in a computational model." J. Comput. Neurosci. 16: 211-35

Terman D., Rubin J., Yew A., Wilson C. (2002). "Activity patterns in a model for the subthalamopallidal network of the basal ganglia." J. Neurosci. 22: 2963-76

Wichman, T., DeLong, M. (2006). "Deep brain stimulation for neurologic and neuropsychiatric disorders." Neuron. 52: 197-204